VOLUME 26 · NUMBER 24 · AUGUST 20 2008

JOURNAL OF CLINICAL ONCOLOGY

BIOLOGY OF NEOPLASIA

New Technologies for Human Cancer Imaging

John V. Frangioni

From the Division of Hematology/Oncology, Department of Medicine, and Department of Radiology, Beth Israel Deaconess Medical Center, Boston, MA.

Submitted September 6, 2007; accepted March 4, 2008.

Supported by Grants No. R01-CA-115296, R01-EB-005805, R21/R33-EB-000673, and R21-CA-129758 from the National Institutes of Health, the Lewis Family Fund, and the Ellison Foundation.

Disclaimers: J.V.F. is named on patents licensed to GE and VisEn Medical. GE and Siemens are subcontractors of the principal investigator on National Institutes of Health grants aimed at optimizing intraoperative near-infrared fluorescence imaging system technology.

Author's disclosures of potential conflicts of interest and author contributions are found at the end of this article.

Corresponding author: John V. Frangioni, MD, PhD, Beth Israel Deaconess Medical Center, 330 Brookline Ave, Rm SL-B05, Boston, MA 02215; e-mail: jfrangio@bidmc.harvard.edu.

0732-183X/08/2624-4012/$20.00

DOI: 10.1200/JCO.2007.14.3065

ABSTRACT

Despite technical advances in many areas of diagnostic radiology, the detection and imaging of human cancer remains poor. A meaningful impact on cancer screening, staging, and treatment is unlikely to occur until the tumor-to-background ratio improves by three to four orders of magnitude (ie, 10^3- to 10^4-fold), which in turn will require proportional improvements in sensitivity and contrast agent targeting. This review analyzes the physics and chemistry of cancer imaging and highlights the fundamental principles underlying the detection of malignant cells within a background of normal cells. The use of various contrast agents and radiotracers for cancer imaging is reviewed, as are the current limitations of ultrasound, x-ray imaging, magnetic resonance imaging (MRI), single-photon emission computed tomography, positron emission tomography (PET), and optical imaging. Innovative technologies are emerging that hold great promise for patients, such as positron emission mammography of the breast and spectroscopy-enhanced colonoscopy for cancer screening, hyperpolarization MRI and time-of-flight PET for staging, and ion beam-induced PET scanning and near-infrared fluorescence-guided surgery for cancer treatment. This review explores these emerging technologies and considers their potential impact on clinical care. Finally, those cancers that are currently difficult to image and quantify, such as ovarian cancer and acute leukemia, are discussed.

J Clin Oncol 26:4012-4021. © 2008 by American Society of Clinical Oncology

INTRODUCTION

There are only six imaging modalities available to clinicians who diagnose, stage, and treat human cancer: x-ray (plain film and computed tomography [CT]), ultrasound (US), magnetic resonance imaging (MRI), single-photon emission computed tomography (SPECT), positron emission tomography (PET), and optical imaging. Of these, only four (CT, MRI, SPECT, and PET) are capable of three-dimensional (3-D) detection of cancer anywhere in the human body.

It is important to understand that the invention and evolution of these imaging modalities were based on historical advances in physics and/or chemistry and not on the needs of oncologists. As will be described, all four 3-D imaging modalities suffer from deficiencies in sensitivity and/or resolution that preclude their ability to solve many of the most important clinical problems in cancer screening, staging, and treatment; they simply were not designed to image small numbers of cancer cells.

The root of the problem is one of scale. A typical cell in the human body is 10 μm in diameter, with a volume of only 1 pL. Hence every 1 cm^3 (1 g) of solid tissue contains approximately 10^9 or one billion cells; the entire human body is estimated to contain approximately 10^{14} cells. Because a malignant clone evolves from a single cell, initially one would need a detectability of 10^{-14}, an inconceivably small number, to detect the genesis of a tumor. However, solid tumors typically display Gompertzian kinetics,[1] with a first lag phase starting from the single cell stage, a log phase heralded by angiogenesis and an escape from diffusion-limited nutrition at approximately the 10^5 cell stage, and a second lag phase culminating in death of the patient at approximately 10^{12} cell (1 kg) stage (Fig 1).

The goal of cancer imaging should be to detect and/or image the smallest possible number of tumor cells, ideally before the angiogenic switch.[2,3] The distinction between what we call detection and imaging is rather arbitrary and is based on the volume element (ie, voxel) size of the particular imaging modality being used. A small collection of tumor cells that is subvoxel in dimensions might be detectable, but because it occupies only a single voxel, a 3-D image is not formed. Regardless of which metric is used, the threshold for detection remains of paramount importance. Unfortunately, as explained in this article, the present detection threshold for solid tumors is approximately 10^9 cells (1 g = 1 cm^3) growing as a single mass. Hence from an imaging

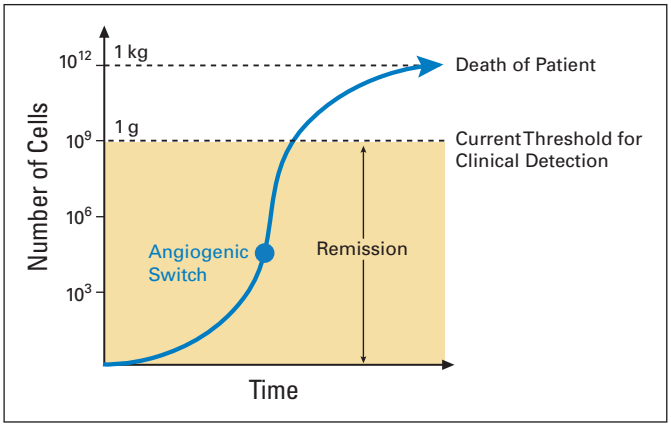

Fig 1. Gompertzian growth curve of a solid tumor and its relationship to cancer detection and imaging. Number of malignant cells (ordinate) as a function of time (abscissa). The transition from first lag to log phase of growth, associated with the transition from diffusion-limited nutrition to neovascularization, is labeled "angiogenic switch." Remission is shown as the uncertainty of cell number ranging from zero to the current clinical threshold for cancer detection (approximately 10^9 cells growing as a single mass).

standpoint, the term remission literally means that there are somewhere between zero and 10^9 malignant cells in the patient's body (Fig 1). This level of uncertainty is unacceptable to both patient and caregiver.

The goal of this review is to inform the reader about why current imaging modalities are generally inadequate for oncology and which new technologies have the potential to improve patient care.

PRINCIPLES OF MEDICAL IMAGING

Signal-to-Background Ratio

Clinical imaging can be essentially reduced to a simple concept: the signal-to-background ratio (SBR), which in the case of cancer imaging is the tumor-to-background ratio. If the goal is to detect or to image cancer cells in the body, then the signal generated by one or more contrast mechanisms must be higher than the background caused by nonspecific signal or nearby normal cells. Even if there is adequate inherent sensitivity and resolution of an imaging modality to detect malignant cells, they will be invisible if the background is too high. To improve the SBR, one of three forms of contrast generation is used: endogenous contrast, exogenous nontargeted contrast, and exogenous targeted contrast.

Endogenous and Nontargeted Exogenous Contrast Agents

Endogenous contrast has undeniable advantages. It doesn't require injection of a contrast agent or costly and time-consuming regulatory approval,[4] and it is generally safe. However, in many clinical situations, endogenous contrast does not provide adequate sensitivity or specificity for detecting malignant cells and their products.

Nontargeted exogenous contrast, typically in the form of an extracellular fluid agent, is used routinely in CT and MRI. After intravenous injection, nontargeted contrast distributes throughout the extracellular space and is cleared rapidly by glomerular filtration. This simple process has been exploited extensively in radiology to indirectly highlight tumors. Because the effects of nontargeted contrast agents are indirect and relatively insensitive, a large number of academic and industrial investigators are developing agents that target malignant cells or their products directly (molecular imaging).

Exogenous Targeted Contrast Agents

The development of cancer-specific diagnostic agents is itself a 3-D problem (Fig 2). The first dimension is affinity (K_D), or more precisely, the ratio of K_D to the concentration of target sites (B_{Max}). The second dimension is biodistribution and clearance, which is a function of the hydrodynamic diameter, charge-to-mass ratio, and hydrophobicity of the contrast agent. Hydrodynamic diameter and charge-to-mass ratio are major determinants of how quickly an agent can extravasate from the vascular space to the malignant cell and how quickly background signal can be cleared from the body. As a general rule, small molecules and peptide ligands (hydrodynamic diameter $\leq$ 3 nm) distribute quickly and clear through the kidneys but require adequate affinity and contact time for effective cancer imaging. Single-chain (hydrodynamic diameter of approximately 5 nm) and full-length antibodies (hydrodynamic diameter of approximately 10 nm) fall on a spectrum from intermediate to poor biodistribution and clearance. Traditional nanoparticles ($\geq$ 10 nm) have virtually no clearance from the body, and even with protective coatings, eventually concentrate in the reticuloendothelial system. A new study from our laboratory has suggested the criteria (the Choi criteria[5]) for the effective use of nanoparticles in vivo. The third dimension is effect size, which for a diagnostic agent is the SBR and for a therapeutic agent is cytotoxicity. Optimizing a contrast agent or radiotracer in all three dimensions is an incredibly difficult task, which presently takes years before clinical testing can even be considered.

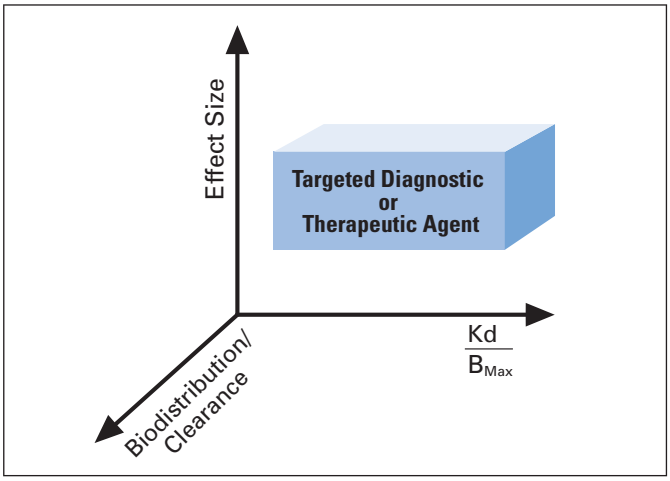

Fig 2. Three-dimensional development of exogenous, targeted diagnostic or therapeutic agents. Colored box delineates optimal in vivo performance.

Additional Barriers to Effective Cancer Imaging

Generating an adequate SBR for detecting/imaging small numbers of malignant cells is made more difficult by the following barriers. First, there is a finite achievable concentration for receptor-targeted agents. The most abundant cancer-associated cell surface targets, such as prostate-specific membrane antigen[6] and Erb-B2,[7] are expressed at approximately 10^5 molecules per cell, corresponding to a cellular concentration of only 170 nmol/L. Most receptors, in fact, are expressed at levels of only 10^3 to 10^4 copies per cell (1.7 to 17 nmol/L). Second, inherent limitations of imaging modality sensitivity and resolution (Table 1) preclude detection or imaging of small numbers of cells. Third, both voluntary and physiologic motion artifacts become increasingly problematic for smaller tumors. Fourth, the body has many barriers to the effective targeting of contrast agents (and therapeutics) in vivo, including inhibitors present in plasma, a relatively small effective endothelial pore size (hydrodynamic diameter of approximately 5 nm) that constrains biodistribution,[5] and basement membranes that act as barriers to preinvasive cancer detection. Finally, many solid tumors have high hydrostatic pressure, which impedes homogeneous infiltration of diagnostic agents.[8,9] Enhanced permeability and retention[10,11] is not discussed in this review because it has questionable relevance to the detection and treatment of preangiogenic small primaries and micrometastases.

CANCER IMAGING MODALITIES

On the basis of its physics and chemistry, each cancer imaging modality has certain limitations with respect to resolution, sensitivity, and contrast generation (Table 1).

US

US uses 1 to 10 MHz sound waves to see inside soft tissue. Because sound waves are highly scattered at bone and air interfaces, many parts of the body are inaccessible, and effective imaging depth is limited in most organs to approximately 10 cm. Although resolution and endogenous contrast are quite high, exogenous contrast in the form of microbubbles must typically be 0.25 to 1 μm in diameter to produce adequate signal. This precludes extravasation from normal vasculature.

X-Ray Imaging

Plain films and CT use the simple principle of shining an x-ray beam through the body and measuring its attenuation. CT rotates the source/detector pair around the patient so that acquired data can be reconstructed into a 3-D image. The main limitation to x-ray imaging is that exogenous contrast agents must have a high atomic number and be at exceptionally high concentrations to attenuate x-rays. The nontargeted, exogenous agents that are currently used clinically are injected at molar

Table 1. Sensitivity and Resolution of Cancer Imaging Modalities as a Function of Cell Number and Contrast Agent/Radiotracer Concentration

Modality	Typical Voxel/Pixel Dimensions (Resolution)	Maximum No. of Cells per Voxel/Pixel	Clinically Available Exogenous Contrast Agent(s)	Radiotracer/ Contrast Agent Hydrodynamic Diameter*	Contrast Agent Concentration per Voxel/Pixel Required for Detection†	No. of Molecules of Contrast per Voxel/Pixel Required for Detection†	Notes
US	1 μL (1×1×1 mm)	10^6	Microbubbles	1 μm	NA	NA	Microbubbles remain intravascular in most tissues
CT	1 μL (1×1×1 mm)	10^6	Iodine	≈1 nm	0.5 M	3×10^{17}	Requirement for molar concentrations precludes targeted imaging
MRI	1 μL (1×1×1 mm)	10^6	Chelated Gd^{3+}	≈1 nm	50 μmol/L	3×10^{13}	Would require > 10^7 Gd^{3+} atoms per cell for detectability
SPECT	1.7 cm^3 (12×12×12 mm)	1.7×10^9	^{99m}Tc ^{111}In ^{67}Ga	≈1 nm	0.3 pM†‡ (≈8×10^3 Bq/voxel)	3×10^8	On average approximately 0.2 radioatoms per cell†‡
PET	0.5 cm^3 (8×8×8 mm)	5×10^8	^{18}F	≈1 nm	0.02 pM†‡ (≈7×10^2 Bq/voxel)	6×10^6	On average approximately 0.01 radioatoms per cell†‡
Optical (2-D)	0.01 mm^2 (0.1×0.1 mm)	10^3	ICG	≈1 nm	≈10-100 nmol/L	6×10^7§	Surface only NIR fluorescence, requires approximately 10^4–10^5 fluorophores per cell for detectability
Optical (3-D)	1 cm^3‖ (1×1×1 cm)	10^9	ICG	≈1 nm	≈10-100 nmol/L	6×10^{13}	NIR tomography-based, requires approximately 10^4–10^5 fluorophores per cell for detectability

Abbreviations: US, ultrasound; NA, not applicable; CT, computed tomography; MRI, magnetic resonance imaging; Gd^{3+}, gadolinium; SPECT, single photon emission computed tomography; ^{99m}Tc, technetium 99m; ^{111}In, indium 111; ^{67}Ga, gallium 67; PET, positron emission tomography; ICG, indocyanine green; NIR, near-infrared.
*After conjugation of a targeting molecule to a contrast agent or radiotracer, final hydrodynamic diameter increases proportionally.
†Does not take into account the significant effect of background and tissue attenuation on detectability. Values shown are theoretical only.
‡Assumes 100 counts, 5 minutes scan, SPECT/PET attenuation of 0.2/0.1, sensitivity of 0.02%/0.5%, half-life of 6/1.8 hours, and maximum specific activity.
§Assuming a tumor thickness of 0.1 mm (10 cells thick).
‖Approximate resolution at a depth of 10 cm in soft tissue such as breast.

concentrations and become invisible after only a few-fold dilution in blood. The generation of targeted CT agents for cancer imaging does not seem technically feasible (Table 1).

MRI

MRI images the small excess in the Boltzmann distribution of spins within the magnetic field. For protons (ie, hydrogen nuclei) at approximately 1.5 T, this excess represents, at most, several parts per million of the total number of hydrogen nuclei present. Because the total proton concentration in most tissue is approximately 80 M, the MRI signal is arising from approximately only 80 μmol/L of the protons present. A major trend in MRI is to improve the signal-to-noise ratio by increasing magnetic field strength from 1.5 T to 3 T and beyond. Because the signal-to-noise ratio scales linearly with field strength, increasing from 1.5 T to 7 T results in an approximately 4.7-fold improvement. Importantly, though, high field strength may introduce other problems, such as increased tissue heating and standing wave patterns present at higher radiowave frequencies.[12]

When intravenously injected gadolinium (Gd^{3+}) -based contrast agents are used, it is not the Gd^{3+} being imaged, but instead, it is the effect of the Gd^{3+} on the magnetic resonance relaxation properties of the protons present in the tissue. This relaxation effect is only observable at concentrations of Gd^{3+} greater than approximately 50 μmol/L, making targeted agents difficult to develop.

SPECT

SPECT is a powerful tool for quantifying the distribution of a radioactive compound (ie, radiotracer) in humans. When a SPECT radioisotope decays, one or more gamma rays (ie, photons), having particular energies, are released in random directions. Because high-energy photons cannot be focused using conventional lenses, collimators are used to restrict the angle of the emitted photons that actually reach the detector. However, typical parallel-hold collimators for SPECT scanners have sensitivities of only approximately 0.02%, that is, only 1/5,000th of the decay events is measured. Also, living tissue is quite effective at attenuating photon energies of SPECT isotopes. Indeed, only 5% of 140 keV technetium 99m (^{99m}Tc) photons remain after traveling 25 cm through the body. When factoring in sensitivity and tissue attenuation, SPECT detects only 1/100,000th of the photons being produced at the cancer site, and the resolution is, at best, $12 \times 12 \times 12$ mm (Table 1).

PET

Positrons, which are antimatter equal in mass but opposite in charge to an electron, are emitted from proton-rich nuclei. Depending on their energy, positrons travel an average distance (the annihilation distance) before interacting with an electron (matter). Although not always appreciated, the density of electrons in a tissue will have a profound effect on the annihilation distance. Less dense tissues, such as lung, have a longer annihilation distance, resulting in lower inherent resolution. The matter (electron) and antimatter (positron) annihilate each other and produce two antiparallel 511-keV photons. Detector crystals are mounted in a stationary ring, and only those 511-keV photons hitting opposing crystals coincidentally are counted.

The overall sensitivity of a clinical PET scanner is approximately 0.5%, and maximal resolution is approximately $8 \times 8 \times 8$ mm (Table 1). Like SPECT isotopes, the body attenuates even 511-keV photons, with only 10% remaining after passage through 25 cm of solid tissue. When factoring in sensitivity and tissue attenuation, PET detects approximately 1/2,000th of the photons being produced at the cancer site. Because of the combined effects of background and tissue attenuation, present PET technology is only capable of detecting solid tumors $\geq 10^9$ cells in size.

Because most PET isotopes are difficult and expensive to synthesize or have extremely short half-lives, they are not routinely available. The exception is fluorine 18 (^{18}F), which has a 110-minute half-life and is available in many chemical forms. The glucose-mimetic 2-deoxy-2-[^{18}F]fluoro-D-glucose (^{18}FDG) is the most commonly used PET compound because it is taken up by metabolically active cells, is not metabolized, and is trapped intracellularly after phosphorylation by hexokinase. Many, but not all, tumors are relatively ^{18}FDG avid (reviewed in Kelloff et al[13]). It is unfortunate that the term PET scanning has come to be a misnomer meaning ^{18}FDG scanning, because ^{18}FDG is only the first and most available ^{18}F contrast agent. It is certainly not an ideal PET radiotracer for cancer imaging, and it has a relatively high uptake in many normal tissues and organs.[14]

Optical Imaging

When a photon of light interacts with living tissue, it can be absorbed or it can be scattered. Thus the two major types of optical imaging are absorption-based and scattering-based. Most optical methods use relatively simple instrumentation to image-reflected excitation light, or fluorescence emission light, from a surface. Tissue reflectance imaging is high resolution (as low as 10 μm) and fast, but because of multiple light scattering, sensitivity is limited by the 1/e optical penetrance, and contrast is derived primarily from superficial structures, typically up to approximately 3 mm in depth. Tomographic optical spectroscopy and imaging (ie, diffuse optics) exploits multiple light scattering and uses computational models to reconstruct the position of absorbing and scattering structures in thick (up to 10 cm) tissues. With the increased imaging depth of diffuse optical imaging, there is a commensurate reduction in resolution compared with superficial imaging methods (Table 1).

NEW IMAGING TECHNOLOGIES FOR CANCER SCREENING

The rationale for screening is to detect cancer before metastasis, and preferably, while the tumor comprises the smallest possible number of cells. Many new technologies suggest dramatic improvements in screening over the next decade.

Breast Cancer Screening

Dedicated CT, positron emission mammography, and dynamic contrast-enhanced MRI. Recent advances in dedicated breast CT technology suggest that 3-D mammograms are now possible, with no more radiation dose than from a two-view mammogram.[15] Although the results of a 45-patient, phase II study are still being analyzed, the addition of intravenous iodine contrast improved detection even further, and tumors that had not been seen with conventional mammography became visible.[16]

Equally exciting is the development of high-resolution, high-sensitivity positron emission mammography (PEM).[17] High background uptake of ^{18}FDG in normal dense breast tissue[14] should not diminish enthusiasm for PEM because improved breast cancer-specific probes are being actively developed.[18] By combining PEM with dedicated CT, or even dynamic contrast-enhanced (DCE) MRI,[19] it should soon be possible to detect tumors as small as 1 mm. However,

whether patients, practitioners, and health care payers will embrace the intravenous injection of one or more diagnostic agents for a revolutionary advance in breast cancer detection remains to be seen.

US and magnetic resonance elastography. In 1991, US-based measurement of soft tissue strain and elastic modulus, termed elastography, was introduced by Ophir et al.[20] Because breast lesions often differ from normal breast tissue in their mechanical properties, elastography was quickly applied to breast nodules.[21] A recent clinical trial comparing US elastography with conventional US and mammography for breast cancer detection showed it to have the highest specificity and lowest false positive rate of the three modalities.[22] Specificity, positive predictive value, and false-positive rate could be improved even further by combining elastography with conventional US imaging.[22] It has also been shown that magnetic resonance can be used to measure the elastic properties of the breast,[23,24] with encouraging initial clinical results in breast cancer detection.[25,26]

Optical. Chance et al[27] introduced endogenous contrast, tomographic near-infrared (NIR) imaging of the human breast in 1994. With this technique, inherent properties of normal and malignant tissue can be probed noninvasively using invisible NIR light. Recent improvements include a handheld device for breast cancer detection[28] and the use of MRI to improve 3-D reconstruction of the optical images.[29] Endogenous contrast optical techniques are attractive for breast cancer screening because they are fast, inexpensive, and safe. The addition of newer, targeted NIR fluorescent contrast agents specific for breast cancer and their microcalcifications[30] could potentially improve sensitivity and specificity even further.

Noncontrast Optical Imaging of Tissue Surfaces

Any accessible tissue surface (eg, the skin, GI tract, and cervix) is amenable to optical imaging, and virtually every variety of noncontrast optical imaging has been studied, including diffuse reflectance,[31] scattering spectroscopy,[32-34] multiwavelength spectroscopy,[35] autofluorescence spectroscopy,[36] and polarization spectroscopy.[37] Although these techniques have different sensitivities to different optical properties of tumors, they all share the major advantages of being fast, safe, and inexpensive. Depending on the precise origin of the contrast, these methods may probe from a few hundred micrometers into the tissue surface up to a few millimeters. Although blood and other endogenous substances can limit light penetration into tissue, hemoglobin sometimes provides an important contrast mechanism. Recent advances in optical coherence tomography, which is capable of providing real-time, near-histology resolution of lumenal surfaces at millimeter depths, promises to be particularly effective for carcinoma screening, especially in the GI tract (reviewed in Brand et al[38] and DaCosta et al[39]).

Contrast-Enhanced Optical Imaging of Tissue Surfaces

The addition of a targeted, exogenous contrast agent, typically in the form of a fluorophore, can improve optical screening of surface tumors significantly. In the case of Barrett's esophagus, the same agent used for a photodynamic therapy response has enough fluorescence yield to provide photodetection of lesion boundaries.[40] A host of other targeted agents for fiberoscopy-based cancer detection have been proposed (reviewed in Wallace et al[41]), with some showing significant promise in preclinical studies.[42]

Virtual Colonoscopy

Over the past 5 years, tremendous progress has been made in virtual colonoscopy using CT (reviewed in Pickhardt and Kim[43]) and MRI (reviewed in Ajaj and Goyen[44]) methods. Although neither technique eliminates the need for a thorough bowel cleansing, both are noninvasive and do not require sedation. In a prospective comparison study, however, the sensitivity of virtual colonoscopy was lower than that of conventional colonoscopy for superficial ulcers and small polyps,[45] and the detection of flat lesions may require fecal tagging or intravenous contrast.[46]

NEW IMAGING TECHNOLOGIES FOR CANCER STAGING

The following innovations aim at improving the detection threshold and/or the quality of human cancer staging.

Replacement of SPECT Radiotracers With PET Radiotracers

Given the multiple technical advantages of PET, an emerging trend is to replace SPECT imaging with PET imaging. The only two factors slowing this transition are the limited availability of the more exotic PET isotopes that are direct replacements for SPECT isotopes and the availability of PET replacements in an appropriate chemical form and half-life appropriate for biodistribution. A particularly attractive isotope for targeted PET imaging is gallium 68 (68-minute half-life), which can be chelated by the same chemical system as indium 111. For example, gallium 68–labeled octreotide imaging of neuroendocrine tumors displayed a 97% sensitivity, a 92% specificity, and an accuracy of 96%,[47] far outperforming two different SPECT octreotide derivatives. Other PET tracers, for which there is no SPECT equivalent, are also being developed at a rapid rate.

Time-of-Flight PET

Traditional PET scanners make no attempt at measuring the extremely small time difference it takes antiparallel photons to reach their respective detectors. Time-of-flight PET scanners measure this time difference and are therefore able to more precisely locate the position of the originating decay event.[48] As a general rule, time-of-flight PET scanners permit the user to choose a two-fold improvement in resolution or a two-fold improvement in sensitivity, but not both. Practical benefits of this performance improvement include achieving cancer detection, which would otherwise fall below the detection threshold, in large patients.[49]

Hyperpolarization MRI

Given the exquisite anatomic imaging capability of MRI, effort has focused on improving its sensitivity to exogenous contrast agents. During the process of hyperpolarization, certain nuclei can be polarized to levels that are between 10^4 and 10^5 times higher than their Boltzmann distribution, enhancing their detectability by MRI. For example, hyperpolarized carbon 13 pyruvate permits high sensitivity detection of tumors in animals.[50] Although the half-life of this improved spin state is typically short, the innovative use of weak magnetic fields[51] and alternative atoms to prolong the effect are exciting avenues of investigation.

Paramagnetic Chemical Exchange Saturation Transfer MRI

At the present time, the only lanthanide used routinely for MRI contrast is Gd^{3+}. However, recent advances in chelation chemistry and MRI pulse sequences exploit additional lanthanides and the

mechanism of paramagnetic chemical exchange saturation transfer (reviewed in Zhang et al[52]). Recent work has improved paramagnetic chemical exchange saturation transfer contrast sensitivity to the 20 to 40 μmol/L range in plasma,[53] with further improvements expected by judicious choice of lanthanide and pulse sequence.

Cancer-Specific Targeting Ligands

A common approach to developing cancer-specific diagnostic agents is to chemically isolate a contrast agent or radiotracer from a separate targeting domain.[54] This modular strategy permits one targeting molecule to create several diagnostic agents for different imaging modalities and vice versa. Investigators have focused on the development of cancer-specific small molecules, single-chain (scFv) antibodies, and other small proteins as targeting molecules (reviewed in Kelloff et al[55]) because immunoglobulin G antibodies have inherent problems in tumor targeting, such as slow biodistribution, slow clearance, and high liver uptake. Recent developments include the multimerization (reviewed in Mammen et al[56]) of small molecules to improve off-rate and affinity[57,58] and the use of yeast antibody display for generating high-affinity scFvs.[59]

Signal Amplification and Background Reduction

To improve the SBR, one can focus on improving the signal, lowering the background, or, ideally, both. Signal amplification is a topic that has attracted considerable attention over the last few years, but few versatile systems have been described. In general, enzymatic amplification achieved by deposition of a contrast agent or radiotracer is flawed because some agents, such as Gd^{3+}, generate no signal in the absence of water, and others, such as radiotracers, can be dose-limiting if deposited in normal organs. A recent innovation in optical imaging, though, is an exception. Kenmoku et al[60] have developed pH-sensitive NIR fluorophores that fluoresce only after receptor-mediated endocytosis, thus greatly reducing background in normal tissues.

NEW IMAGING TECHNOLOGIES FOR CANCER TREATMENT

Image-guided therapy offers a glimpse into the era of so-called personalized medicine. The following technologies can assist the clinician in making patient-specific decisions aimed at improving the delivery of cancer treatment.

Image-Guided Chemotherapy

^{18}FDG-PET, ^{99m}Tc-Annexin, DCE-MRI, and optical tomography have all been shown to be effective in monitoring the response of tumors to chemotherapy. Recent prospective clinical trials using ^{18}FDG-PET in non–small-cell lung cancer,[61] esophageal cancer,[62] and lymphoma[63] have demonstrated that scans obtained 1 to 3 weeks after initiation of therapy are predictive not only of response, but also of improved overall survival. ^{99m}Tc-labeled Annexin V in conjunction with SPECT imaging was also predictive of treatment response in a wide variety of tumors.[64-66] For breast cancer chemotherapy, both DCE-MRI[67] and optical spectroscopy[68] have proven effective in the neoadjuvant setting. The fundamental problem with all of these methods, though, is quantitative assessment of log kill.

Image-Guided Ion Beam Radiotherapy

Proton and carbon ion beam therapies, and their associated Bragg peaks, not only target tumors more precisely, but also produce in situ positrons at the site of energy delivery. These positrons can then

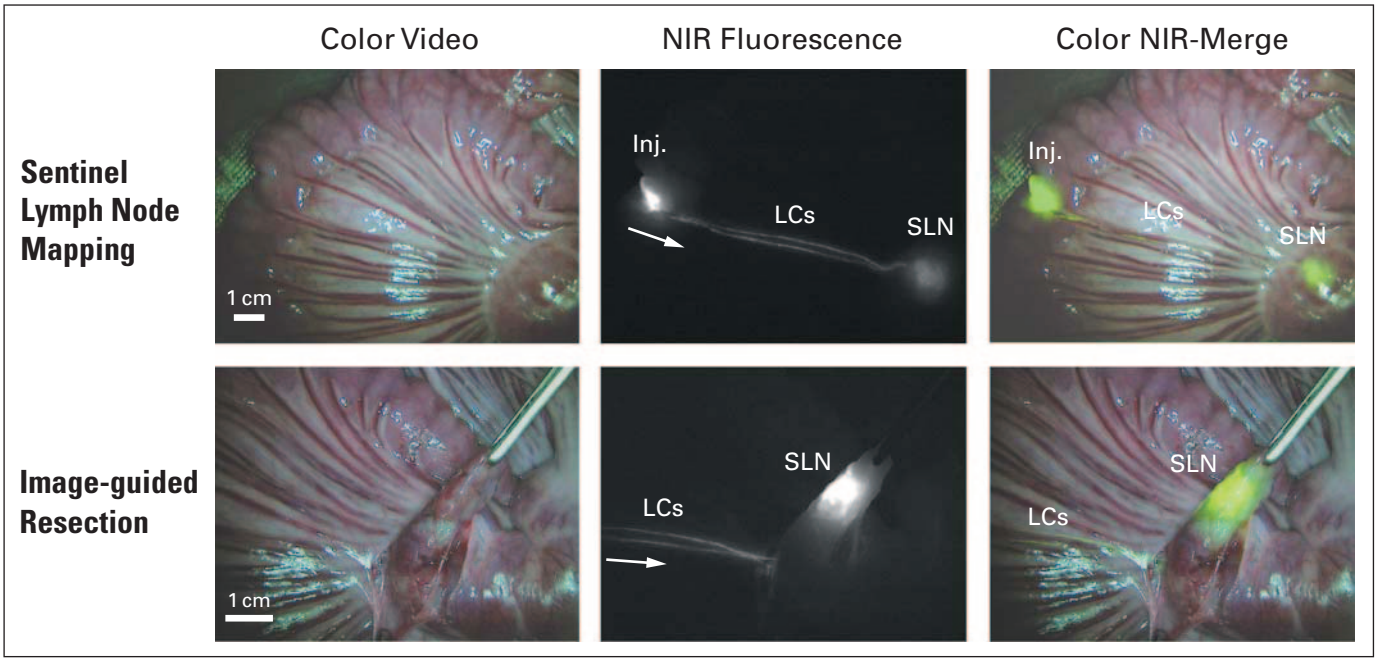

Fig 3. Intraoperative image-guidance using invisible near-infrared (NIR) fluorescent light. Indocyanine green (ICG) mixed with human serum albumin (HSA) creates a sensitive lymphatic tracer (ICG:HSA)[74] of 7 nm in hydrodynamic diameter. After injection (Inj) into the parenchyma of swine colon, lymphatic channels (LCs) are seen within seconds, and within 1 to 2 minutes, the sentinel lymph node (SLN) has been identified (top) and can be resected under image guidance (bottom). Shown for each are the color video (left), 800-nm NIR fluorescence (middle), and merged images (pseudocolored in green; right) of the two. Arrow shows the direction of lymph flow. All images are refreshed at 15 Hz using a previously described intraoperative NIR fluorescence imaging system.[72]

Table 2. New Technologies for Human Cancer Imaging

Clinical Problem	Cancer/Discipline	New Technology	Advantage	Disadvantage	Reference
Screening	Breast	Dedicated CT	High resolution and sensitivity	Ionizing radiation (same as 2-view mammogram)	15,16
		PEM	High sensitivity, moderate to high resolution	Requires IV injection of radiotracer	17
		DCE-MRI	High resolution and specificity	Requires IV injection of lanthanide chelate	19
		Diffuse optical tomography (spectroscopy)	Noncontrast study, safe, 3-D, quantitative, high specificity, can be combined with MRI	Low resolution, low to moderate sensitivity	27-29
	Endoscopy/colonoscopy/ colposcopy	Optical (diffuse reflectance)	Fast, inexpensive, safe	Surface imaging only, interference from blood	31
		Optical (photon scattering)	Fast, inexpensive, safe	Surface imaging only, interference from blood	32-34
		Optical (multi-wavelength spectroscopy)	Fast, inexpensive, safe	Surface imaging only, interference from blood	35
		Optical (autofluorescence spectroscopy)	Fast, inexpensive, safe	Surface imaging only, interference from blood	36
		Optical (polarization spectroscopy)	Fast, inexpensive, safe	Surface imaging only, interference from blood	37
		Optical coherence tomography	Fast, high resolution, safe	Limited depth to ≈ 2 mm, endogenous contrast only	38,39
		Exogenous fluorescence	High sensitivity and specificity	Requires IV injection of contrast agent	40-42
	Virtual colonoscopy	CT-based	Noninvasive, relatively fast	Uses ionizing radiation, difficulty with flat lesions and small polyps	43
		MRI-based	Noninvasive, relatively fast	Difficulty with flat lesions and small polyps	44
Staging	PET	Replacements for SPECT radiotracers	Higher sensitivity and resolution	Desired half-life not always available	47
		Time-of-flight detection	2-fold higher resolution or sensitivity	Limited availability	48,49
	MRI	Hyperpolarization	High sensitivity possible, in vivo tracking of molecule metabolism	Relatively short relaxation times of agents tested to date	50,51
		PARACEST	Higher sensitivity than traditional lanthanide imaging	Sensitivity not yet adequate for receptor-based imaging	53
	All	Low-molecular weight targeting ligands	Rapid biodistribution and clearance	Tumor contact time often inadequate	54-59
		Signal amplification/background reduction (optical)	Improved SBR	Requires endocytosis and pH-dependent activation	60
Treatment	Chemotherapy	Image-guided treatment (^{18}FDG-PET)	Highly sensitive	Expensive, not all tumors FDG-avid, difficult to quantify log kill	61-63
		Image-guided treatment (^{99m}Tc-Annexin V)	Moderately sensitive	Presently unavailable, difficult to quantify log kill	64-66
		Image-guided treatment (DCE-MRI)	No ionizing radiation	Requires intravenous injection of lanthanide chelate, difficult to quantify log kill	67
		Image-guided treatment (optical spectroscopy)	No ionizing radiation, fast, safe, quantitative, high sensitivity and specificity	Low resolution, moderate sensitivity, difficult to quantify log kill	68
	Radiotherapy	Ion beam-induced PET and PET/CT	Near real-time feedback on dose delivery	Requires specialized and expensive infrastructure, difficult mathematical modeling	69
	Surgery	Optical (reflectance NIR fluorescence)	Fast, real-time, high sensitivity and specificity	Poor depth penetration (≈1-3 mm)	70-72,79,81, 82,84
		Optical (tomographic NIR fluorescence)	Depth penetration up to several cm, quantitative, high specificity	Requires separate acquisition and reconstruction, low to moderate resolution, low to moderate sensitivity	73

Abbreviations: CT, computed tomography; PEM, positron emission mammography; IV, intravenous; DCE, dynamic contrast-enhanced; MRI, magnetic resonance imaging; SPECT, single photon emission computed tomography; PARACEST, paramagnetic chemical exchange saturation transfer; SBR, signal-to-background ratio; ^{18}FDG, 2-deoxy-2-[^{18}F]fluoro-D-glucose; ^{99m}Tc, technetium 99m; NIR, near-infrared.

be used to image and quantify radiotherapy delivery using PET or PET/CT scanning.[69] 3-D feedback of ion beam therapy is under intense investigation and promises significant improvements in the precision of dose delivery.

Image-Guided Surgery

The only two imaging techniques used even occasionally during oncologic surgery are x-ray fluoroscopy (for angiography) and US (for mass detection). However, the former exposes patients and caregivers to ionizing radiation, the latter requires direct contact with tissue, and neither can be used with targeted contrast agents. Optical imaging that exploits invisible NIR fluorescent light (700 to 900 nm) offers several advantages for image-guided surgery, including low inherent autofluorescence background, highly sensitive and specific detection of tumors up to millimeters deep in scattering tissue, and real-time imaging (reviewed in Frangioni[70]). Intraoperative imaging systems developed by our laboratory also provide simultaneous acquisition of surgical anatomy (color video) and function (NIR fluorescence).[71,72] Innovative work from other groups has extended depth penetration to several centimeters using frequency-domain photon migration (optical tomography) techniques.[73]

Presently, the only clinically available NIR fluorophore is indocyanine green, which is a nontargeted extracellular fluid agent approved for nonfluorescence indications. Nevertheless, by simply mixing indocyanine green with human serum albumin, a highly fluorescent 7-nm (hydrodynamic diameter) complex is formed,[74] which can be used for NIR fluorescent sentinel lymph node mapping of virtually any tissue or organ (Fig 3).[72,75-78] Many investigators are also developing NIR fluorophores targeted specifically to human cancer and normal structures.[79-83] If translated to the clinic, these targeted NIR fluorescent contrast agents would permit the oncologic surgeon to resect malignant cells under direct visualization while actively avoiding critical structures such as vessels and nerves.

IMAGING DIFFICULT CANCERS

Even with some of the new technologies described earlier, certain types of cancer will remain inherently difficult to detect and image.

Ovarian Cancer

Ovarian cancer arises from a monolayer of flat-to-cuboidal cells called the ovarian surface epithelium; hence the earliest proliferative lesion is only approximately 10 μm thick. As such, early-stage ovarian cancer, and even small metastases, are difficult to image using conventional technology. Optical imaging, though, is especially well suited for sensitive and rapid interrogation of large surfaces. Penson et al[84] at Fox Chase Cancer Center have shown that intravenous injection of indocyanine green in conjunction with a specially designed laparoscope could permit image-guided debulking of peritoneal metastases. It is intriguing to speculate whether such technology might also someday aid in the screening of high-risk populations.

Acute Leukemia

Recent evidence points to a so-called stem-cell niche in the bone marrow that is required for sustenance of acute leukemia.[85] Although the bone marrow is well vascularized, which aids in contrast agent biodistribution to the target cells, the small number of malignant and normal cells comprising the niche, the need for signal amplification, and most important, high background from normal bone marrow cells make detection and imaging of leukemic stem cells extremely difficult.

Pediatric Cancer

There are only approximately 12,000 total cases of cancer in children age 0 to 18 years each year in the United States, comprising dozens of types and subtypes.[86] Although there are a few successful diagnostic agents used routinely in clinical care,[87] small market sizes and difficulties in performing clinical trials contribute to significant unmet need in this patient population.

SUMMARY AND CONCLUSIONS

A summary of the new technologies for human cancer imaging that have been discussed in this review is provided in Table 2. In sum, the detection and imaging of small numbers of cancer cells anywhere in the human body remains elusive. Although new technologies, such as optical imaging, will likely play an important role in certain clinical applications, the field of oncology needs a revolutionary advance in the physics and chemistry of tumor detection.

At what detection threshold will molecular imaging have a major impact on overall survival? Although arbitrary, a reasonable goal for the ensuing decade would be the detection and imaging of small primaries or small metastases that are just below the volume associated with the angiogenic switch. Because tumor spheroids can sustain growth by diffusion until a diameter of approximately 1 mm,[2,3] this would correspond to approximately 5.2×10^5 cells. Interestingly, reaching this detection threshold would have an immediate impact on unsolved clinical problems in other fields of medicine, for instance, the detection of small numbers of stem cells during disease therapy[88] and the quantitation of pancreatic β-cell islets during the progression of diabetes.[89]

Finally, there is little difference between the molecular imaging of human cancer and the molecular therapy of human cancer; the 3-D nature of the two is the same (Fig 2). If a contrast agent or radiotracer can someday be targeted to a living cancer cell anywhere in the body, then a cytotoxic agent can be targeted as well. In fact, the smaller the detected tumor, the more options that will be available to kill it. It is this synergy between imaging and treatment that provides hope for the future of clinical oncology.

AUTHOR'S DISCLOSURES OF POTENTIAL CONFLICTS OF INTEREST

Although all authors completed the disclosure declaration, the following author(s) indicated a financial or other interest that is relevant to the subject matter under consideration in this article. Certain relationships marked with a "U" are those for which no compensation was received; those relationships marked with a "C" were compensated. For a detailed description of the disclosure categories, or for more information about ASCO's conflict of interest policy, please refer to the Author Disclosure Declaration and the Disclosures of Potential Conflicts of Interest section in Information for Contributors.

Employment or Leadership Position: None **Consultant or Advisory Role:** None **Stock Ownership:** None **Honoraria:** None **Research Funding:** John V. Frangioni, GE Healthcare **Expert Testimony:** None **Other**

Remuneration: John V. Frangioni, Royalties from Beth Israel Deaconess Medical Center

REFERENCES

1. Norton L, Simon R, Brereton HD, et al: Predicting the course of Gompertzian growth. Nature 264:542-545, 1976

2. Groebe K, Mueller-Klieser W: On the relation between size of necrosis and diameter of tumor spheroids. Int J Radiat Oncol Biol Phys 34:395-401, 1996

3. Naumov GN, Akslen LA, Folkman J: Role of angiogenesis in human tumor dormancy: Animal models of the angiogenic switch. Cell Cycle 5:1779-1787, 2006

4. Frangioni JV: Translating in vivo diagnostics into clinical reality. Nat Biotechnol 24:909-913, 2006

5. Choi HS, Liu W, Misra P, et al: Renal clearance of quantum dots. Nat Biotechnol 25:1165-1170, 2007

6. Smith-Jones PM, Vallabahajosula S, Goldsmith SJ, et al: In vitro characterization of radiolabeled monoclonal antibodies specific for the extracellular domain of prostate-specific membrane antigen. Cancer Res 60:5237-5243, 2000

7. Hernández-Sotomayor SM, Arteaga CL, Soler C, et al: Epidermal growth factor stimulates substrate-selective protein-tyrosine-phosphatase activity. Proc Natl Acad Sci U S A 90:7691-7695, 1993

8. Boucher Y, Leunig M, Jain RK: Tumor angiogenesis and interstitial hypertension. Cancer Res 56:4264-4266, 1996

9. Boucher Y, Jain RK: Microvascular pressure is the principal driving force for interstitial hypertension in solid tumors: Implications for vascular collapse. Cancer Res 52:5110-5114, 1992

10. Matsumura Y, Oda T, Maeda H: [General mechanism of intratumor accumulation of macromolecules: Advantage of macromolecular therapeutics]. Gan To Kagaku Ryoho14:821-829, 1987

11. Maeda H, Matsumura Y: Tumoritropic and lymphotropic principles of macromolecular drugs. Crit Rev Ther Drug Carrier Syst 6:193-210, 1989

12. Hoult DI, Phil D: Sensitivity and power deposition in a high-field imaging experiment. J Magn Reson Imaging 12:46-67, 2000

13. Kelloff GJ, Hoffman JM, Johnson B, et al: Progress and promise of FDG-PET imaging for cancer patient management and oncologic drug development. Clin Cancer Res 11:2785-2808, 2005

14. Kumar R, Chauhan A, Zhuang H, et al: Standardized uptake values of normal breast tissue with 2-deoxy-2-[F-18]fluoro-D: -glucose positron emission tomography: Variations with age, breast density, and menopausal status. Mol Imaging Biol 8:355-362, 2006

15. Boone JM, Lindfors KK: Breast CT: Potential for breast cancer screening and diagnosis. Future Oncol 2:351-356, 2006

16. Boone JM, Kwan AL, Yang K, et al: Computed tomography for imaging the breast. J Mammary Gland Biol Neoplasia 11:103-111, 2006

17. Weinberg IN: Applications for positron emission mammography. Phys Med 21:132-137, 2006 (suppl 1)

18. Hofmann M: From scinti-mammography and metabolic imaging to receptor targeted PET-new principles of breast cancer detection. Phys Med 21:11, 2006 (suppl 1)

19. Dougherty L, Isaac G, Rosen MA, et al: High frame-rate simultaneous bilateral breast DCE-MRI. Magn Reson Med 57:220-225, 2007

20. Ophir J, Cespedes I, Ponnekanti H, et al: Elastography: A quantitative method for imaging the elasticity of biological tissues. Ultrason Imaging 13: 111-134, 1991

21. Céspedes I, Ophir J, Ponnekanti H, et al: Elastography: Elasticity imaging using ultrasound with application to muscle and breast in vivo. Ultrason Imaging 15:73-88, 1993

22. Zhi H, Ou B, Luo BM, et al: Comparison of ultrasound elastography, mammography, and sonography in the diagnosis of solid breast lesions. J Ultrasound Med 26:807-815, 2007

23. Plewes DB, Bishop J, Samani A, et al: Visualization and quantification of breast cancer biomechanical properties with magnetic resonance elastography. Phys Med Biol 45:1591-1610, 2000

24. Sinkus R, Lorenzen J, Schrader D, et al: High-resolution tensor MR elastography for breast tumour detection. Phys Med Biol 45:1649-1664, 2000

25. Van Houten EE, Doyley MM, Kennedy FE, et al: Initial in vivo experience with steady-state subzone-based MR elastography of the human breast. J Magn Reson Imaging 17:72-85, 2003

26. Lorenzen J, Sinkus R, Lorenzen M, et al: MR elastography of the breast: Preliminary clinical results. Rofo 174:830-834, 2002

27. Nioka S, Miwa M, Orel S, et al: Optical imaging of human breast cancer. Adv Exp Med Biol 361:171-179, 1994

28. Hsiang D, Shah N, Yu H, et al: Coregistration of dynamic contrast enhanced MRI and broadband diffuse optical spectroscopy for characterizing breast cancer. Technol Cancer Res Treat 4:549-558, 2005

29. Carpenter CM, Pogue BW, Jiang S, et al: Image-guided optical spectroscopy provides molecular-specific information in vivo: MRI-guided spectroscopy of breast cancer hemoglobin, water, and scatterer size. Opt Lett 32:933-935, 2007

30. Bhushan KR, Tanaka E, Frangioni JV: Synthesis of conjugatable bisphosphonates for molecular imaging of large animals. Angew Chem Int Ed Engl 46:7969-7971, 2007

31. Georgakoudi I, Van Dam J: Characterization of dysplastic tissue morphology and biochemistry in Barrett's esophagus using diffuse reflectance and light scattering spectroscopy. Gastrointest Endosc Clin N Am 13:297-308, 2003

32. Kim YL, Turzhitsky VM, Liu Y, et al: Low-coherence enhanced backscattering: Review of principles and applications for colon cancer screening. J Biomed Opt 11:041125, 2006

33. Lovat LB, Johnson K, Mackenzie GD, et al: Elastic scattering spectroscopy accurately detects high grade dysplasia and cancer in Barrett's oesophagus. Gut 55:1078-1083, 2006

34. Perelman LT: Optical diagnostic technology based on light scattering spectroscopy for early cancer detection. Expert Rev Med Devices 3:787-803, 2006

35. Orfanoudaki IM, Themelis GC, Sifakis SK, et al: A clinical study of optical biopsy of the uterine cervix using a multispectral imaging system. Gynecol Oncol 96:119-131, 2005

36. Huh WK, Cestero RM, Garcia FA, et al: Optical detection of high-grade cervical intraepithelial neoplasia in vivo: Results of a 604-patient study. Am J Obstet Gynecol 190:1249-1257, 2004

37. Arrazola P, Mullani NA, Abramovits W: DermLite II: An innovative portable instrument for dermoscopy without the need of immersion fluids. Skinmed 4:78-83, 2005

38. Brand S, Poneros JM, Bouma BE, et al: Optical coherence tomography in the gastrointestinal tract. Endoscopy 32:796-803, 2000

39. DaCosta RS, Wilson BC, Marcon NE: Optical techniques for the endoscopic detection of dysplastic colonic lesions. Curr Opin Gastroenterol 21:70-79, 2005

40. Kennedy JC, Marcus SL, Pottier RH: Photodynamic therapy (PDT) and photodiagnosis (PD) using endogenous photosensitization induced by 5-aminolevulinic acid (ALA): Mechanisms and clinical results. J Clin Laser Med Surg 14:289-304, 1996

41. Wallace MB, Sullivan D, Rustgi AK: Advanced imaging and technology in gastrointestinal neoplasia: Summary of the AGA-NCI Symposium October 4-5, 2004. Gastroenterology 130:1333-1342, 2006

42. Alencar H, Funovics MA, Figueiredo J, et al: Colonic adenocarcinomas: Near-infrared microcatheter imaging of smart probes for early detection—Study in mice. Radiology 244:232-238, 2007

43. Pickhardt PJ, Kim DH: CT colonography (virtual colonoscopy): A practical approach for population screening. Radiol Clin North Am 45:361-375, 2007

44. Ajaj W, Goyen M: MR imaging of the colon: "technique, indications, results and limitations". Eur J Radiol 61:415-423, 2007

45. Abdel Razek AA, Abu Zeid MM, Bilal M, et al: Virtual CT colonoscopy versus conventional colonoscopy: A prospective study. Hepatogastroenterology 52:1698-1702, 2005

46. Park SH, Lee SS, Choi EK, et al: Flat colorectal neoplasms: Definition, importance, and visualization on CT colonography. AJR Am J Roentgenol 188: 953-959, 2007

47. Gabriel M, Decristoforo C, Kendler D, et al: 68Ga-DOTA-Tyr3-octreotide PET in neuroendocrine tumors: Comparison with somatostatin receptor scintigraphy and CT. J Nucl Med 48:508-518, 2007

48. Cherry SR: The 2006 Henry N. Wagner Lecture: Of mice and men (and positrons)—Advances in PET imaging technology. J Nucl Med 47:1735-1745, 2006

49. Surti S, Kuhn A, Werner ME, et al: Performance of Philips Gemini TF PET/CT scanner with special consideration for its time-of-flight imaging capabilities. J Nucl Med 48:471-480, 2007

50. Golman K, Zandt RI, Lerche M, et al: Metabolic imaging by hyperpolarized 13C magnetic resonance imaging for in vivo tumor diagnosis. Cancer Res 66:10855-10860, 2006

51. Jonischkeit T, Bommerich U, Stadler J, et al: Generating long-lasting 1H and 13C hyperpolarization in small molecules with parahydrogen-induced polarization. J Chem Phys 124:201109, 2006

52. Zhang S, Merritt M, Woessner DE, et al: PARACEST agents: Modulating MRI contrast via water proton exchange. Acc Chem Res 36:783-790, 2003

53. Vinogradov E, He H, Lubag A, et al: MRI detection of paramagnetic chemical exchange effects in mice kidneys in vivo. Magn Reson Med 58:650-655, 2007

54. Humblet V, Misra P, Frangioni JV: An HPLC/mass spectrometry platform for the development of multimodality contrast agents and targeted therapeutics: Prostate-specific membrane antigen small molecule derivatives. Contrast Media Mol Imaging 1:196-211, 2006

55. Kelloff GJ, Krohn KA, Larson SM, et al: The progress and promise of molecular imaging probes

in oncologic drug development. Clin Cancer Res 11:7967-7985, 2005

56. Mammen M, Choi SK, Whitesides GM: Polyvalent interactions in biological systems: Implications for design and use of multivalent ligands and inhibitors. Angew Chem Int Ed Engl 37:2754-2794, 1998

57. Handl HL, Vagner J, Han H, et al: Hitting multiple targets with multimeric ligands. Expert Opin Ther Targets 8:565-586, 2004

58. Misra P, Humblet V, Pannier N, et al: Production of multimeric prostate-specific membrane antigen small-molecule radiotracers using a solid-phase 99mTc preloading strategy. J Nucl Med 48:1379-1389, 2007

59. Graff CP, Chester K, Begent R, et al: Directed evolution of an anti-carcinoembryonic antigen scFv with a 4-day monovalent dissociation half-time at 37 degrees C. Protein Eng Des Sel 17:293-304, 2004

60. Kenmoku S, Urano Y, Kojima H, et al: Development of a highly specific rhodamine-based fluorescence probe for hypochlorous acid and its application to real-time imaging of phagocytosis. J Am Chem Soc 129:7313-7318, 2007

61. Nahmias C, Hanna WT, Wahl LM, et al: Time course of early response to chemotherapy in non-small cell lung cancer patients with 18F-FDG PET/CT. J Nucl Med 48:744-751, 2007

62. Lordick F, Ott K, Krause BJ, et al: PET to assess early metabolic response and to guide treatment of adenocarcinoma of the oesophagogastric junction: The MUNICON phase II trial. Lancet Oncol 8:797-805, 2007

63. Kelloff GJ, Sullivan DM, Wilson W, et al: FDG-PET Lymphoma Demonstration Project Invitational Workshop. Acad Radiol 14:330-339, 2007

64. Rottey S, Slegers G, Van Belle S, et al: Sequential 99mTc-hydrazinonicotinamide-annexin V imaging for predicting response to chemotherapy. J Nucl Med 47:1813-1818, 2006

65. Kartachova M, Haas RL, Olmos RA, et al: In vivo imaging of apoptosis by 99mTc-Annexin V scintigraphy: Visual analysis in relation to treatment response. Radiother Oncol 72:333-339, 2004

66. Kartachova M, van Zandwijk N, Burgers S, et al: Prognostic significance of 99mTc Hynic-rh-annexin V scintigraphy during platinum-based chemotherapy in advanced lung cancer. J Clin Oncol 25:2534-2539, 2007

67. Chou CP, Wu MT, Chang HT, et al: Monitoring breast cancer response to neoadjuvant systemic chemotherapy using parametric contrast-enhanced MRI: A pilot study. Acad Radiol 14:561-573, 2007

68. Cerussi A, Hsiang D, Shah N, et al: Predicting response to breast cancer neoadjuvant chemotherapy using diffuse optical spectroscopy. Proc Natl Acad Sci U S A 104:4014-4019, 2007

69. Nishio T, Ogino T, Nomura K, et al: Dose-volume delivery guided proton therapy using beam on-line PET system. Med Phys 33:4190-4197, 2006

70. Frangioni JV: In vivo near-infrared fluorescence imaging. Curr Opin Chem Biol 7:626-634, 2003

71. De Grand AM, Frangioni JV: An operational near-infrared fluorescence imaging system prototype for large animal surgery. Technol Cancer Res Treat 2:553-562, 2003

72. Tanaka E, Choi HS, Fujii H, et al: Image-guided oncologic surgery using invisible light: Completed pre-clinical development for sentinel lymph node mapping. Ann Surg Oncol 13:1671-1681, 2006

73. Reynolds JS, Troy TL, Mayer RH, et al: Imaging of spontaneous canine mammary tumors using fluorescent contrast agents. Photochem Photobiol 70:87-94, 1999

74. Ohnishi S, Lomnes SJ, Laurence RG, et al: Organic alternatives to quantum dots for intraoperative near-infrared fluorescent sentinel lymph node mapping. Mol Imaging 4:172-181, 2005

75. Knapp DW, Adams LG, Degrand AM, et al: Sentinel lymph node mapping of invasive urinary bladder cancer in animal models using invisible light. Eur Urol 52:1700-1708, 2007

76. Parungo CP, Colson YL, Kim SW, et al: Sentinel lymph node mapping of the pleural space. Chest 127:1799-1804, 2005

77. Parungo CP, Ohnishi S, Kim SW, et al: Intraoperative identification of esophageal sentinel lymph nodes with near-infrared fluorescence imaging. J Thorac Cardiovasc Surg 129:844-850, 2005

78. Parungo CP, Soybel DI, Colson YL, et al: Lymphatic drainage of the peritoneal space: A pattern dependent on bowel lymphatics. Ann Surg Oncol 14:286-298, 2007

79. Figueiredo JL, Alencar H, Weissleder R, et al: Near infrared thoracoscopy of tumoral protease activity for improved detection of peripheral lung cancer. Int J Cancer 118:2672-2677, 2006

80. Humblet V, Lapidus R, Williams LR, et al: High-affinity near-infrared fluorescent small-molecule contrast agents for in vivo imaging of prostate-specific membrane antigen. Mol Imaging 4:448-462, 2005

81. Ke S, Wen X, Gurfinkel M, et al: Near-infrared optical imaging of epidermal growth factor receptor in breast cancer xenografts. Cancer Res 63:7870-7875, 2003

82. Li C, Wang W, Wu Q, et al: Dual optical and nuclear imaging in human melanoma xenografts using a single targeted imaging probe. Nucl Med Biol 33:349-358, 2006

83. Tanaka E, Ohnishi S, Laurence RG, et al: Real-time intraoperative ureteral guidance using invisible near-infrared fluorescence. J Urol 178:2197-2202, 2007

84. Penson R, Horowitz N, Kassis E, et al: Laparoscopy in the near infrared with ICG detects microscopic tumor in women with ovarian cancer. Presented at Annual Meeting of the Society for Molecular Imaging, Big Island, HI, August 30 to September 2, 2006

85. Jin L, Hope KJ, Zhai Q, et al: Targeting of CD44 eradicates human acute myeloid leukemic stem cells. Nat Med 12:1167-1174, 2006

86. Ries LAG, Melbert D, Krapcho M, et al: SEER Cancer Statistics Review, 1975-2004, Section XX-VIII, Childhood Cancer by Site, Incidence, Survival and Mortality. Bethesda, MD, National Cancer Institute, 2007. http://seer.cancer.gov/csr/1975_2004/

87. Pashankar FD, O'Dorisio MS, Menda Y: MIBG and somatostatin receptor analogs in children: Current concepts on diagnostic and therapeutic use. J Nucl Med 46:55S–61S, 2005 (suppl 1)

88. Frangioni JV, Hajjar RJ: In vivo tracking of stem cells for clinical trials in cardiovascular disease. Circulation 110:3378-3383, 2004

89. Sweet IR, Cook DL, Lernmark A, et al: Non-invasive imaging of beta cell mass: A quantitative analysis. Diabetes Technol Ther 6:652-659, 2004

Acknowledgment

I thank Aya Matsui, MD, and Joshua H. Winer, MD, for images from near-infrared fluorescent sentinel lymph node mapping, Robert E. Lenkinski, PhD, J. Anthony Parker, MD, PhD, and Bruce J. Tromberg, PhD, for critical reading of the manuscript, Barbara L. Clough for editing, and Eugenia Trabucchi for administrative assistance.

